

# A Pore-Flow-Through Membrane Reactor for Partial Hydrogenation of 1,5-Cyclooctadiene

**A. Schmidt**

Technische Universität Berlin, Institut für Chemie, Straße des 17. Juni 124, D-10623 Berlin, Germany

**A. Wolf and R. Warsitz**

Bayer Technology Services GmbH, D-51368 Leverkusen, Germany

**R. Dittmeyer and D. Urbanczyk**

Karl-Winnacker-Institut, DECHEMA e.V., Theodor-Heuss-Allee 25, D-60486 Frankfurt, Germany

**I. Voigt and G. Fischer**

Hermisdorfer Institut für Technische Keramik HITK e.V., Michael-Faraday-Str. 1, D-07629 Hermisdorf, Germany

**R. Schomäcker**

Technische Universität Berlin, Institut für Chemie, Straße des 17. Juni 124, D-10623 Berlin, Germany

DOI 10.1002/aic.11379

Published online November 30, 2007 in Wiley InterScience (www.interscience.wiley.com).

*The partial hydrogenation of 1,5-cyclooctadiene was performed in a pore-flow-through membrane reactor at 50°C and 1 MPa hydrogen pressure with single capillary membranes and a bundle of 27 capillaries for scale-up studies. A preparation method for the catalytically active membranes and their characterization are described. Compared to millimeter-sized spherical catalyst pellets in fixed-bed or slurry reactors, mass transfer limitations could be successfully reduced in the membrane reactor. The conversion rate of 1,5-cyclooctadiene in the membrane reactor was mainly affected by the Pd amount and the mass flow rate of the reaction mixture through the membrane. Under optimum conditions a selectivity of 95% for cyclooctene at complete conversion of 1,5-cyclooctadiene was obtained. This value corresponds to the selectivity obtained with a powder catalyst with a particle size of approx. 25 µm in a slurry reactor for which microkinetic control of the reaction is expected to result in the highest possible selectivity. © 2007 American Institute of Chemical Engineers AIChE J, 54: 258–268, 2008*

*Keywords: hydrogenation, three-phase reaction, pore diffusion, selectivity, catalytic membrane, membrane reactor*

## Introduction

Hydrogenation reactions in liquid phase are very common in chemical industry. Mostly they are heterogeneously cata-

lyzed as a solid catalyst is easy to separate from the reaction mixture. A frequently met disadvantage of such three-phase reactions arises from mass transport limitations that reduce activity and selectivity. Firstly, the hydrogen has to be transferred from the gas phase into the liquid phase. On industrial scale this problem is mostly solved by increased hydrogen pressure and intense stirring in an autoclave. Secondly, the reactants in the liquid phase must be transported into the

Correspondence concerning this article should be addressed to A. Schmidt at schomaecker@tu-berlin.de.

pores of the solid catalyst and, after reaction at the active centers, the reactants and the products must be removed fast enough before side reactions occur. In the case of consecutive reactions, mass transport phenomena like pore diffusion and back mixing within the reactor increase the effective rate of the consecutive reaction and decrease the selectivity for the desired product. With a very fine catalyst powder, pore diffusion can be widely eliminated, but for an industrial application powders are often not adequate due to the difficulty to separate them from the product: costly and time-consuming filtration steps would be necessary. Egg-shell catalysts have been developed to solve this problem where a support, spherical or of other shapes, is coated with a very thin layer of the catalytically active metal. In this way, effects of pore diffusion inside the catalyst particle can be minimized, but the size and geometry of egg-shell catalysts have to be adjusted to every reaction considered.<sup>1</sup> A recently developed concept to reduce the influence of pore diffusion is to pump the reaction mixture fast enough through the pores of a membrane in which the catalyst is immobilized on the pore walls. With a flow velocity of  $10^{-3}$  m s<sup>-1</sup>, the convective flow of the reactants is at least one order of magnitude faster than the diffusional displacement of the molecules in the liquid phase which is of the order of  $10^{-5}$  m within 1 s. This results in residence times well below 1 s for the reaction mixture within the membrane pores.

In the studied case, porous inorganic membranes serve as a support material for catalytically active Pd-nanoparticles. They allow an efficient contact between catalyst and reactants but do not cause separation problems of the catalyst.<sup>1-3</sup>

It is also possible to use catalytic membranes with asymmetric geometry for keeping gas and liquid phase separate, feeding both reactants from opposite sides of the membrane.<sup>4-7</sup> In recent years, several studies on the performance of membrane reactors in hydrogenation reactions have been published.<sup>1-15</sup> The concepts for suppressing undesired side reactions by reaction engineering in a membrane reactor is transferable to other reactions and other membrane materials (e. g. dimerization,<sup>16</sup> Fischer-Tropsch synthesis,<sup>17</sup> dehalogenation,<sup>5,16</sup> nitrate/nitrite reduction,<sup>7</sup> dehydrogenation,<sup>11</sup> and oxidation.<sup>20</sup> For partial hydrogenation reactions of polyunsaturated hydrocarbons, the application of a pore-flow-through (PFT) membrane reactor is well described. In a previous study<sup>2</sup> we reported that the selectivity for the partially hydrogenated product can be increased by using a PFT membrane reactor compared to slurry and fixed bed reactors with catalyst pellets. Following the results of this previous work, the investigations in this paper are focused on the partial hydrogenation of 1,5-cyclooctadiene in a PFT membrane reactor where the consecutive reaction to the fully hydrogenated product cyclooctane should be avoided. This reaction was selected as a representative example for a variety of partial hydrogenation reactions of polyunsaturated hydrocarbons, like natural oils, terpenes, or substances with triple bonds that need to be transferred to double bonds. Its kinetic parameters are in a typical range of rate and adsorption constants for this type of reactions. Single tubular alumina membranes (capillaries) containing Pd nanoparticles were chosen for a first series of experiments studying the influence of different process parameters. The scale up of the PFT membrane reactor was investigated in a pilot plant equipped with

an assembled bundle of 27 capillaries, and the results were compared to the experiments with single capillaries.

Different characterization methods for the palladium distribution on the ceramic support are described. As the solubility of hydrogen in the liquid phase is modest, the reaction mixture had to be resaturated and pumped several times through the membrane in order to obtain complete conversion of the diene. The results of the hydrogenation in the membrane reactor are compared to experiments in a slurry reactor and a fixed bed reactor with a commercial Pd/alumina catalyst to evaluate the potential of the membrane reactor.

## Experimental

Single tubular membranes and bundles with 27 assembled capillaries made of porous  $\alpha$ -Al<sub>2</sub>O<sub>3</sub> (produced by Hermsdorfer Institut für Technische Keramik, Hermsdorf, Germany) were used as support material for the palladium catalyst. The capillaries had a length of 250 mm, an outer diameter of 2.9 mm, and an inner diameter of 1.9 mm. Membranes with three different nominal pore diameters (0.6, 1.9, and 3.0  $\mu$ m) were studied. The membrane pores were loaded with palladium by wet impregnation with aqueous precursor solutions. Membrane properties (pore diameter, porosity ca. 30%) were not changed by the Pd deposition.

Pd deposition on the membranes was accomplished by wet impregnation with an aqueous PdCl<sub>2</sub> (99.9%, Alfa Aesar)-solution (19 mmol/L), circulated with a flow rate of 80 mL/min for 24 h through the membrane, and subsequent activation by reduction to Pd with NaH<sub>2</sub>PO<sub>2</sub>H<sub>2</sub>O (=99%, Fluka)-solution (59 mmol/L) for 1 h at room temperature. After washing with water and drying at room temperature, the membranes were catalytically active (Figure 1). Characterization of the catalytically active membranes involved atomic absorption spectroscopy (AAS), scanning electron microscopy (SEM), transmission electron microscopy (TEM), and electron probe micro analysis (EPMA).

Catalytic experiments were performed for partial hydrogenation of 1,5-cyclooctadiene (COD) to cyclooctene (COE) in a reactor system in PFT mode. The reactor system (Figure 2) consisted of a saturation vessel and a membrane reactor module connected in a loop. The membrane module can accommodate up to three single capillaries; its temperature is controlled through a heating jacket. The stainless steel vessel has a capacity of 130 mL and is equipped with a gas dispersion stirrer and baffles. All experiments were performed with a total liquid volume of 110 mL of which about 45 mL resided in the membrane module including pipes and the remaining 65 mL in the saturation vessel. The vessel is mounted in an oil bath with a temperature control unit. The circulation rate of the reaction mixture through the reactor system can be set by a gear pump in the range between 50 and 350 mL/min. Samples of the reaction mixture were taken during the experiment and analyzed by gas chromatography, using a Siemens Sichromat 3 equipped with a Restek RTX 5 MS column. The experiments were carried out in semibatch mode employing *n*-heptane as solvent. Hydrogen was fed to the system from a reservoir with the desired initial hydrogen pressure. A computer monitored the decrease of the hydrogen pressure in the reservoir during the reaction online.

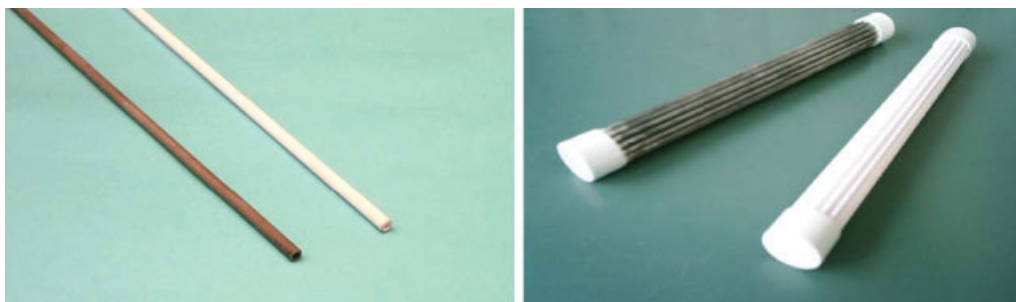


**Figure 1.**  $\alpha$ -Al<sub>2</sub>O<sub>3</sub> supports and Pd-membranes, (left) single capillary and (right) capillary bundle.

[Color figure can be viewed in the online issue, which is available at [www.interscience.wiley.com](http://www.interscience.wiley.com).]

The pilot plant for the capillary bundles (membrane area: 0.054 m<sup>2</sup>) was constructed similar to the lab scale but in a larger dimension at Bayer Technology Services, Leverkusen, Germany. The saturation vessel has a capacity of 5 L, it was temperature controlled by a thermostat. All experiments were performed with a liquid inventory of about 3 L. The circulation rate of the reaction mixture was varied from 5 to 11 L/min by a gear pump. The hydrogen pressure in the saturation vessel was kept constant during the reaction. After a saturation time of 15 min the reaction was started by turning on the pump. Samples of the reaction mixture were taken in intervals of 10 min and analyzed by GC.

For benchmarking, additional hydrogenation experiments were performed with a commercially available egg-shell catalyst (Pd/ $\gamma$ -alumina, 0.5 wt % Pd, spherical pellets, pellet size 2–3 mm) in a fixed bed reactor. For these experiments, the membrane module in the laboratory set up was replaced by a fixed bed reactor. The system was operated at a circulation rate of 200 mL/min. Additional experiments for benchmarking were performed with a powder catalyst in a stainless

steel autoclave (capacity 130 mL) equipped with a gas dispersion stirrer and baffles. Hydrogen was fed into the reactor at constant pressure. The autoclave was heated to the desired temperature by a heating jacket. A commercial Pd/ $\alpha$ -Al<sub>2</sub>O<sub>3</sub> catalyst (0.5 wt % Pd) was ground and sieved to a particle size below 25  $\mu$ m.

Both catalysts were investigated by low temperature nitrogen adsorption (POROTEC Sorptomatic 1990) to detect the specific surface area and by carbon monoxide pulse chemisorption (POROTEC TPDRO 1100) to determine the Pd surface area. The Pd/ $\alpha$ -Al<sub>2</sub>O<sub>3</sub> powder catalyst showed a specific surface area of 8 m<sup>2</sup>/g and a Pd surface area of 0.7–1.1 m<sup>2</sup>/g corresponding to a Pd particle size of about 2.3–3.8 nm (spheres), whereas the specific surface area for the egg-shell Pd/ $\gamma$ -Al<sub>2</sub>O<sub>3</sub> catalyst was 245 m<sup>2</sup>/g and the Pd surface area 2.0–2.9 m<sup>2</sup>/g indicating very small Pd particles with an average diameter of ca. 0.9–1.3 nm (spheres). The Pd containing zone in the egg-shell catalyst was  $\sim$ 100  $\mu$ m thick.

The experiments were carried out with 1,5-cyclooctadiene in *n*-heptane with initial COD concentration of 5 vol % at 50°C, hydrogen pressure of 1 MPa and a Pd amount of 1.0 mg (200 mg of supported catalyst) suspended in 110 mL solution of COD in *n*-heptane. The stirrer speed was adjusted to 1600 rpm for all experiments in order to assure fast saturation of the solution. Gas-liquid mass transport was characterized by a  $k_L a$ -value of 0.15 s<sup>-1</sup>.

## Modeling

Mathematical models were developed in Matlab<sup>®</sup> (The Mathworks, Release 2007a) to assist the interpretation of the experimental results. The kinetics of the reaction is described according to a recently published kinetic model for COD hydrogenation on a Pd/ $\alpha$ -Al<sub>2</sub>O<sub>3</sub> catalyst.<sup>18</sup> The reaction rate constants are based on the metal surface area to take into account the differences in Pd dispersion. The loop reactor is modeled as a two component system consisting of a well-mixed saturator vessel and a one-dimensional flow-through reactor. For the reactor a pseudo-stationary assumption is introduced, i.e., it is assumed that the time for a significant change of the concentrations in the saturator (the reactor inlet concentrations) is large compared to the residence time of the fluid passing through the membrane. Moreover, the membrane capillary is considered as a homogeneous system with equally distributed catalyst, i.e., ignoring the diffusion across the pore diameter as well as the diffusion in direction of the

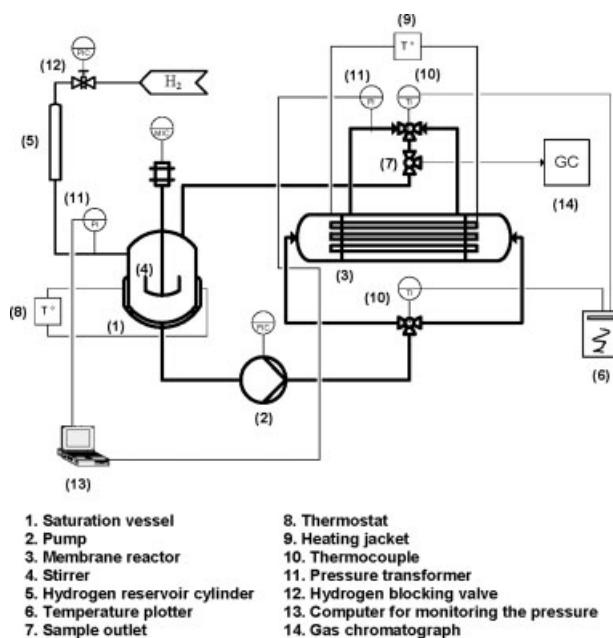


**Figure 2.** Scheme of the reactor system for single tube membranes.

pore axis (plug flow). This leads to a system of ordinary differential equations for the reactor which is solved for time-invariant initial conditions by the routine ODE45 (4th/5th order variable step size Runge-Kutta method). With the resulting concentrations in the reactor effluent, the concentrations in the saturator vessel are updated by integration of the material balances for the saturator over time making use of a similar 5th order Runge-Kutta method with adaptive step size control.<sup>19</sup> The calculations begin with the known concentrations in the saturator at  $t = 0$ ; they are terminated at a defined end time or when complete conversion is reached. The model provides the time-dependent concentrations in the saturator vessel and in the reactor effluent as well the time-dependent spatial concentration profiles inside the catalytic membrane.

The assumption of negligible diffusion resistance across the pore radius was verified by a two-dimensional simulation of convection and diffusion in the pores and the catalyzed reaction at the pore walls performed with FEMLAB (Comsol AB, Release 3.0). Straight cylindrical pores of radius  $d_p/2$  and length  $(d_a - d_i)/2\tau$  were assumed, where  $d_p$  is the nominal pore diameter,  $d_a$  and  $d_i$  denote the outer and the inner diameter of the capillary, respectively, and  $\tau$  is the tortuosity which was arbitrarily set to 2. The reaction was included in the definition of the boundary condition as a flux term assuming equal distribution of the catalyst over the whole pore wall area. Only small concentration changes from the center of the pore to the pore wall are predicted for the conditions of interest, e.g., pore diameters between 0.6 and 3  $\mu\text{m}$  as well as the geometries and flow rates of the systems described in this article, which have no significant impact on the reaction rate.

For simulation of the benchmarking experiments, an additional pseudo-stationary one-dimensional heterogeneous model was developed which simulates a packed-bed of spherical egg-shell catalyst pellets based on a cascade of well-mixed cells. Each cell contains a certain amount of solid catalyst and liquid as given by the bed voidage. The porous catalyst is treated as a homogeneous medium using constant effective diffusivities of the various species based on an assumed porosity of 0.6 and tortuosity of 2. A dimensionless sigmoidal distribution function for the active material over the pellet radius,  $f = \tanh(2\pi s[x - x_0])$ , was introduced to enable the simulation of an egg-shell catalyst. Here  $x_0$  is a dimensionless radius coordinate marking the inner border of the active shell ( $0 \leq x_0 \leq 1$ ), and  $s$  is a steepness parameter which was arbitrarily set to 50. The Pd loading in the active region of the pellet is found by dividing the average Pd loading of the pellet by the integral of  $f$  over the radius of the sphere. The external mass transfer resistance at the pellet surface is neglected because of the high flow velocity of the liquid phase. The resulting system of second-order ordinary differential equations for coupled reaction and diffusion inside the catalyst is solved by the routine BVP4C (multipoint boundary value problem solver). To determine the cell's exit concentrations in the liquid, an iterative strategy is used where the concentrations are repeatedly updated with the fluxes derived from the concentration gradients at the pellet surface based on the material balances for the pseudo-stationary well-mixed cell until the changes become negligible.

The heterogeneous model also served to simulate the experiments with the powder catalyst in the slurry reactor.

This is possible by setting the number of cells to one and including hydrogen uptake from the gas phase in the hydrogen material balance for the cell. Moreover, the catalyst distribution function is set to  $f = 1$  and the geometrical parameters of the system (particle diameter, solid-phase volume per cell) are adjusted.

## Results

### Membrane characterization

The Pd amount in the membranes was determined by AAS (PERKIN-ELMER 3500). Before AAS-measurements, the Pd was dissolved from the membrane with 10 mL of aqua regia. The amount of Pd per membrane varied from 0.7 to 1.5 mg with an average Pd content of 1 mg (0.038 wt %). The Pd loading could not be increased significantly above that level, e.g. by using higher Pd concentrations of the impregnation solution or by repetition of the impregnation process. The AAS-measurements were accomplished for a number of membranes prepared under the same conditions. In addition, some membranes were analyzed by AAS after the hydrogenation experiments. The accuracy of the detected Pd amounts on single capillaries is estimated at  $\pm 0.1$  mg. Leaching of Pd could be excluded based on AAS analyses of the product of the hydrogenation experiments without dilution (Pd detection limit 3.6  $\mu\text{g/L}$ ).

The Pd amounts deposited on capillary bundles were determined by weighing before and after the impregnation and drying; in this way Pd amounts of 29–35 mg were detected with an estimated accuracy of  $\pm 1$  mg.

The Pd particle size of the catalytic membranes was studied by TEM. TEM micrographs of Pd crystallites on alumina particles from various membranes showed crystallite sizes ranging from 5 to 15 nm with an ensemble average of about 8.5 nm. No significant influence of the pore size of the capillaries on the Pd crystallite size could be detected (Table 1). TEM analyses from a membrane used for hydrogenation experiments showed the same results as for freshly impregnated membranes. This indicates that the Pd particles do not undergo obvious changes during the reaction.

The distribution of Pd over the cross-section of the capillaries was analyzed by electron probe microanalysis (EPMA) on a CAMECA SX50 instrument equipped with four crystal spectrometers with an electron beam of 15 kV  $\times$  30 nA. The beam diameter was 3  $\mu\text{m}$ ; its penetration depth into the material was about 5  $\mu\text{m}$  (Figure 3a). Specimens were prepared by cutting a capillary, grinding, and polishing on a STRUERS ROTOSYSTEM. The grinding was carried out with SiC paper of 220, 320, 500, 1000, and 2400 grit successively under a press of 80 N. The grinding time for each step was 1 min. Polishing was done for 5 min under a press of 80 N on an MDMol substrate (STRUERS) with a suspension of 3- $\mu\text{m}$ -grade diamond, and then on a MD-Nap substrate (STRUERS) with a suspension of 1- $\mu\text{m}$ -grade diamond. The polished specimens were treated with graphite for electrical conductivity.

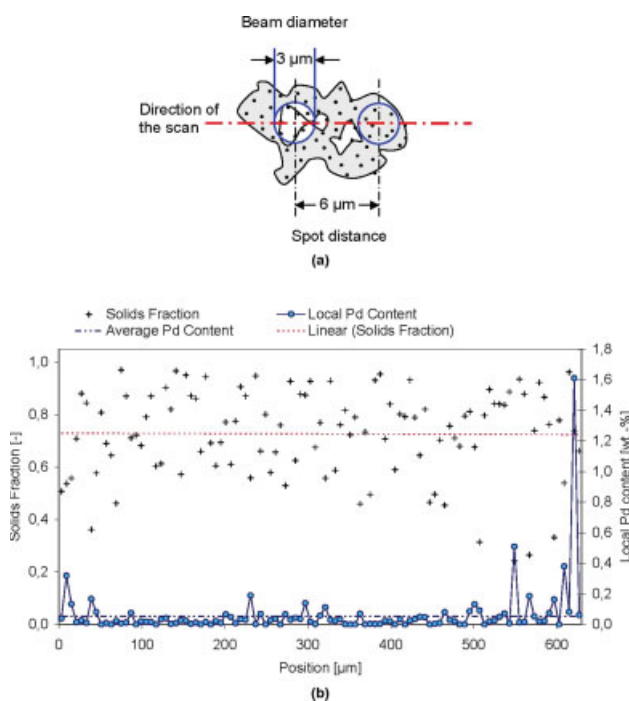
Three cross-sectional cuts were prepared from two pieces close to the ends and one from the middle of a 25 cm long single capillary with 1.9  $\mu\text{m}$  pore diameter loaded with 1.5 mg Pd. In each cross section two adjacent line scans over the whole wall were recorded. Figure 3b shows the

**Table 1. Average Pd Particle Sizes at Different Membranes**

Membrane	I	II	III	IV
Pore diameter of membrane ( $\mu\text{m}$ )	0.6	1.9	3.0	1.9
Average size of Pd particle (nm)	$9.4 \pm 1.3$	$7.8 \pm 2.7$	$9.0 \pm 1.4$	$7.6 \pm 1.4$

I-III prepared only for TEM, IV after hydrogenation experiment with COD.

measured Pd content along one of these line scans. There is a large scattering of the local Pd content, but the data reveal that the Pd is uniformly distributed over the wall. Two main factors contribute to the scattering: The measuring volume is of the same order of magnitude as the pore size. This leads to a greatly varying fraction of void space in the measuring volume from point to point (Figure 3b). The Pd particles are located on the surface of the large alumina particles. So for a spot with a large fraction of voids in the measuring volume the instrument detects a higher Pd to Al ratio than for a spot with no voids (Figure 3a). This is confirmed by a correlation between the local Pd content and the solids fraction detected in the measuring volume for all scans. Because of the presence of void space, the average Pd content is derived from a line scan as the ratio of the total amount of Pd detected vs. the total amount of solids ( $\text{Al}_2\text{O}_3$  and Pd) (Table 2). In addition to the void space, the Pd particle size distribution influences the scattering: Large peaks of the local Pd content may be caused by large agglomerated Pd particles randomly found in the measuring volume.

**Figure 3. Pd content measured by EPMA over the membrane cross section.**

(a) Variation of the solids fraction from point to point. (b) Local Pd content and fraction of solids along a line scan over the wall of the capillary. [Color figure can be viewed in the online issue, which is available at [www.interscience.wiley.com](http://www.interscience.wiley.com).]

**Table 2. Pd Contents Derived from EPMA Line Scans from Different Parts of a Single Capillary**

	Scan1	Scan2	Part of the Membrane
Average Pd amount in wt%	0.053	0.124	End
	0.047	0.041	Middle
	0.045	0.074	End

The average Pd content of the capillary derived from all six line scans is  $0.064 \pm 0.032$  wt % which corresponds to a Pd loading of  $1.65 \pm 0.82$  mg. Thus, agreement with the amount of 1.5 mg expected from the preparation is satisfactory.

### Partial hydrogenation in membrane reactor

The potential of the membrane reactor in PFT mode for the partial hydrogenation of COD (Figure 4) was first tested with single capillary membranes by varying the circulation rate of the reactants through the membrane and the pore size of the membrane. Also a variation of the Pd amount of the capillaries in the range of 0.7–1.5 mg occurred. The influence of these parameters on the reaction rate and the selectivity for COE was investigated at  $50^\circ\text{C}$ , 1 MPa  $\text{H}_2$ -pressure and a COD concentration of 5 vol % in *n*-heptane.

The following definitions are used for describing the performance of the membrane reactor:

$$\text{Conversion of COD: } X(\%) = \frac{C_{\text{COD},0} - C_{\text{COD},t}}{C_{\text{COD},0}} \times 100 \quad (1)$$

$$\text{Selectivity for COE: } S(\%) = \frac{C_{\text{COE},t}}{C_{\text{COD},0} - C_{\text{COD},t}} \times 100 \quad (2)$$

In Figure 5a the conversion of COD obtained with a membrane with  $1.9 \mu\text{m}$  pore size and a Pd loading of 1.5 mg is plotted as a function of time for 4 different circulation rates. With increasing circulation rate from 80 to 260 mL/min, the time for complete conversion of COD decreases from 80 to 40 min. However, a higher circulation rate means an increased pressure drop over the membrane, in particular for small pore size (Figure 6). Figure 5b shows the selectivity for COE at different circulation flow rates. The selectivity stays close to 100% for up to 60% conversion and then decreases to 92–95% at complete conversion. Apparently, there is no influence of the circulation rate on the selectivity.

In Figure 7a the time dependent conversion for the hydrogenation on membranes with different pore sizes under the same reaction conditions is shown. The reaction is clearly faster for the membrane with  $0.6 \mu\text{m}$  pore size than for the membranes with larger pore diameters of 1.9 and  $3.0 \mu\text{m}$ . However, as evident from Figure 7b the selectivity for COE is unaffected by the pore size. It reaches 98% at 80% COD conversion and 93–95% at complete conversion, which is very close to the data shown in Figure 5.

From Figure 8a, a strong influence of the Pd loading on the reaction rate becomes obvious. Three membranes with 0.7, 1.0, and 1.5 mg Pd per membrane are compared for COD hydrogenation at the same circulation rate, temperature and hydrogen pressure. With increasing Pd loading, the reaction is clearly accelerated. However, the effect detected in the experiments is larger than predicted by the simulation model. Dou-



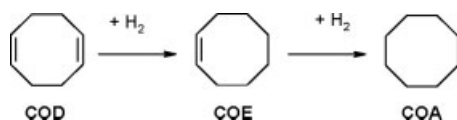


**Figure 4.** Reaction scheme of 1,5-COD hydrogenation.

bling of the Pd loading of the membrane theoretically leads to doubling of the reaction rate, if there is no significant decrease of the reactant concentration within the membrane. The observed as well as the predicted selectivity is not affected by the Pd loading of the membrane (Figure 8b).

### Comparison of different reactor systems

In Figure 9a the conversion of COD in three different reactor configurations is compared under similar reaction conditions at 50°C, 1 MPa hydrogen pressure and 1 mg Pd content: membrane (0.038 wt % Pd, pore diameter: 1.9  $\mu\text{m}$ ), Pd/ $\gamma$ -alumina egg shell catalyst (0.5 wt % Pd, particle size: 2-3 mm) in fixed-bed reactor, and Pd/ $\alpha$ -alumina powder catalyst (0.5 wt % Pd, particle size <25  $\mu\text{m}$ ) in slurry reactor. The COD hydrogenation experiments in the fixed-bed and in the slurry reactor serve for benchmarking the performance of the catalytic membranes. The Pd amount was kept at 1 mg in all experiments. In the slurry reactor the liquid phase is expected to be saturated with hydrogen at any time of the reaction. This follows from the measured volumetric gas-liquid mass transfer coefficient ( $k_{\text{La}} = 0.15 \text{ s}^{-1}$ ).<sup>3</sup> Under these conditions, the powder catalyst reached an initial reaction rate of 0.039 mol/(g<sub>Pd</sub> s). Almost the same initial rate was obtained with the catalytic membrane [0.035 mol/(g<sub>Pd</sub> s)], which is understandable from the simulation results in Figure 9: a moderate decrease of the hydrogen concentration upon passing through the membrane is expected for the chosen conditions, so that the membrane operates under microkinetic control. In contrast, the initial rate for the egg shell catalyst in the fixed-bed reactor was 0.021 mol/(g<sub>Pd</sub> s). According to micrographs taken from several broken pellets, the thickness of the active shell in this catalyst varies randomly from about 50 to 300  $\mu\text{m}$ . Figure 10 also shows the simulation results

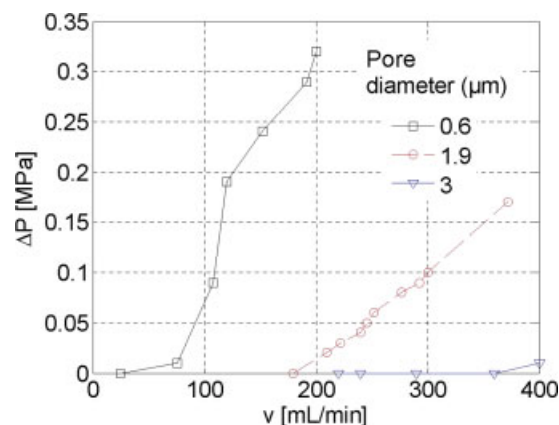
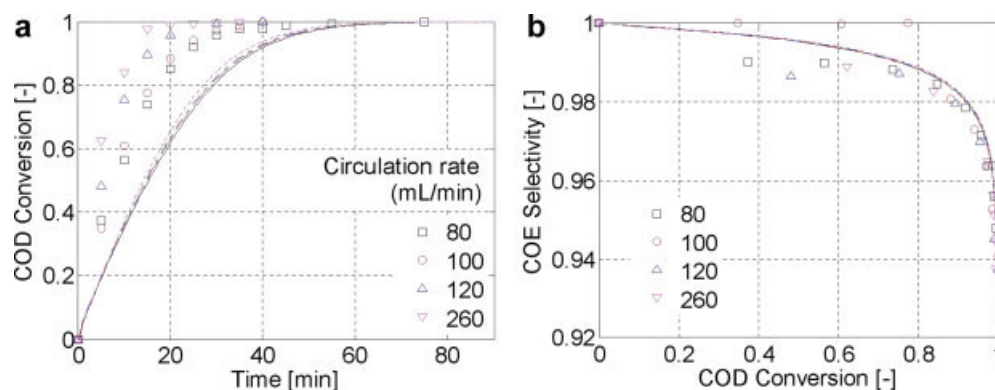


**Figure 6.** Pressure drop at membrane for different circulation flow rates and pore sizes; measured with single capillaries and *n*-heptane at 25°C.

[Color figure can be viewed in the online issue, which is available at [www.interscience.wiley.com](http://www.interscience.wiley.com).]

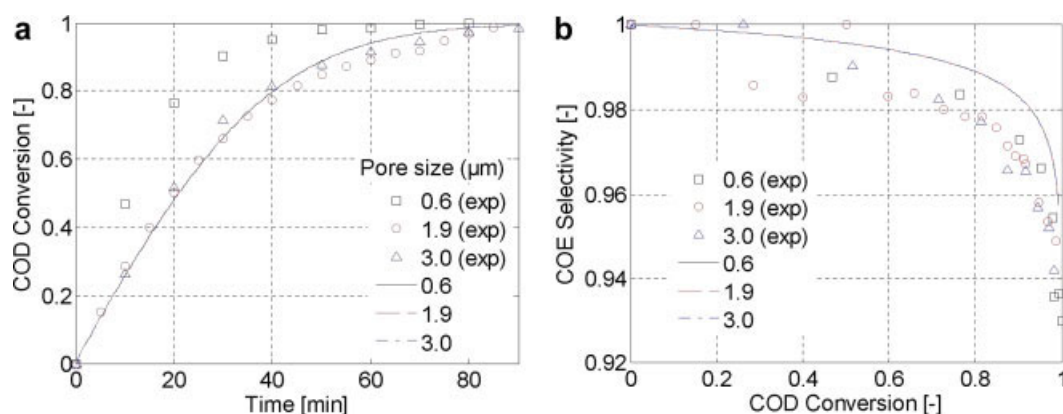
for two assumed (uniform) thicknesses of the active shell, i.e., 100  $\mu\text{m}$  ( $x_0 = 0.92$ ) and 200  $\mu\text{m}$  ( $x_0 = 0.84$ ). Clearly, the simulation results are highly sensitive to the shell thickness, which suggests a strong influence of pore diffusion limitation on the reaction rate for the egg shell catalyst. In the light of the moderate scattering in the rates measured for the catalytic membranes in the studies of the long term stability, this is no considerable difference between egg shell catalyst and catalytic membrane.

Figure 9b compares the selectivity for COE obtained in the different reactors. With the powder catalyst a selectivity of 95% at complete conversion is obtained; the membrane reached a similar selectivity of 94% which also indicates the absence of mass transfer effects on the reaction rate. With the egg shell catalyst in the fixed bed reactor, a substantially lower selectivity for COE is obtained at complete conversion (45%). This indicates accumulation of COE in the pores because of pore diffusion limitation promoting the consecutive reaction to COA.



**Figure 5.** Conversion (a) and selectivity for COE (b) for different circulation rates with a membrane with 1.9  $\mu\text{m}$  pore diameter (50°C, 1 MPa  $\text{H}_2$ -pressure, 5 vol % COD, Pd loading:  $1.5 \pm 0.1$  mg, symbols: experimental data, lines: simulation results).

[Color figure can be viewed in the online issue, which is available at [www.interscience.wiley.com](http://www.interscience.wiley.com).]



**Figure 7. Conversion (a) and selectivity to COE (b) for membranes with different pore size (50°C, 1 MPa H<sub>2</sub>-pressure, Pd loading:  $1 \pm 0.1$  mg, circulation rate: 200 mL/min, symbols: experimental data, lines: simulation results).**

[Color figure can be viewed in the online issue, which is available at [www.interscience.wiley.com](http://www.interscience.wiley.com).]

### Long-term performance of the catalytic membranes

A series of measurements under the same conditions (50°C, 1 MPa H<sub>2</sub>-pressure, circulation flow rate 200 mL/min) was carried out with a membrane with 1.9  $\mu\text{m}$  pore size to study the possible loss of activity with increasing number of experiments. In Figure 10a, the time dependent conversion is plotted for 6 out of 11 experiments. There is some fluctuation within these results, but no systematic degradation of the performance. Instead for all experiments a reaction time of 70–80 min for complete conversion is observed. The selectivity for COE is also barely affected; the values are in the range of 92–94% at complete conversion (Figure 10b).

Insofar, only little deactivation of the catalyst is observable. AAS analysis of the product did not reveal any Pd leaching. The long-term stability was also proved for the 27-membrane bundle in the pilot plant in 10 consecutive hydrogenation experiments.

However, an increase of the pressure difference at the membrane from 0.05 to 0.4 MPa at a constant flow rate of 260 mL/min was observed in lab scale. TOC (total organic carbon) measurements on membranes used for hydrogenation experiments revealed an increased carbon content (0.07–0.15

wt %) compared to new membranes (0–0.01 wt %) which indicates some coking of the catalyst during the reaction. Although apparently not (yet) affecting the activity of the membrane, an increase of the pressure drop is undesirable as it increases the demand for pump energy. Therefore, measures for regenerating the membrane have to be found. The easiest way would be to rinse the membranes by flushing them with solvent. This was tested for single capillaries with *n*-heptane and acetone but did not show any success. By contrast regeneration was possible by calcining the membranes for 2 h at 300°C in air and then activating them for 2 h at 250°C in hydrogen flow. After this procedure the membrane showed an unchanged activity, and the pressure difference was decreased to the same level as for freshly prepared membranes (0.1–0.2 MPa at 260 mL/min).

### Scale-up of membrane reactor

For any industrial application scale-up of the reactor system to larger dimensions is necessary. For the experiments in the pilot plant, assembled bundles of 27-capillary membranes were used. Further scale-up is possible by mounting several of these bundles, preferably with increased length of about

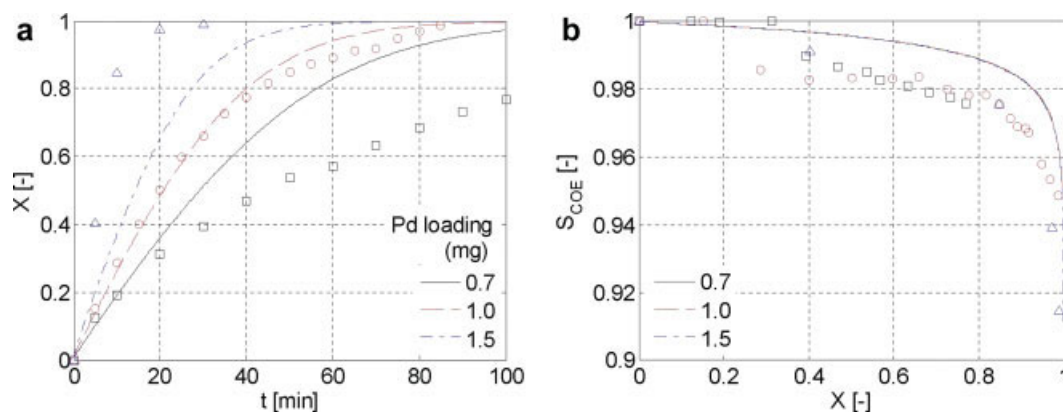


**Figure 8. Conversion (a) and selectivity (b) as a function of the Pd loading of the membrane (50°C, 1 MPa H<sub>2</sub> pressure, pore size: 1.9  $\mu\text{m}$ , circulation rate: 200 mL/min, symbols: experimental data, lines: simulation results).**

[Color figure can be viewed in the online issue, which is available at [www.interscience.wiley.com](http://www.interscience.wiley.com).]

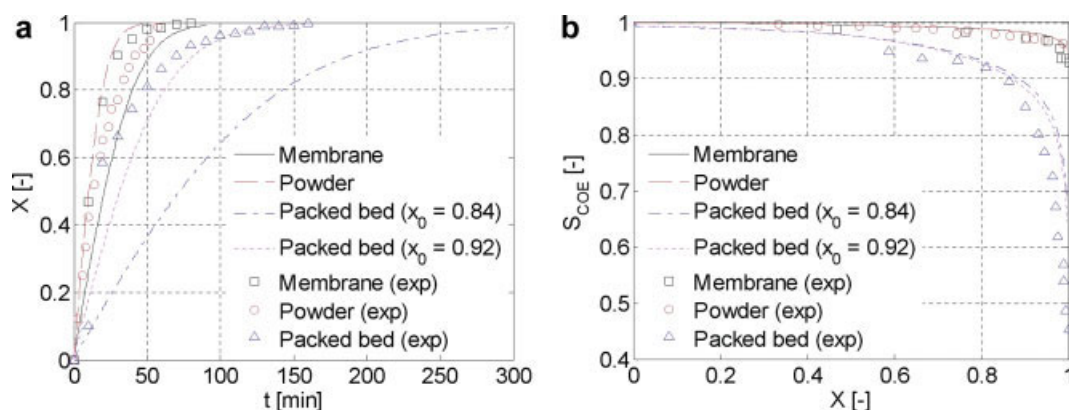


**Figure 9.** COD-conversion (a) and COE-selectivity (b) for different types of catalysts: PFT membrane reactor (1 mg Pd, circulation rate: 200 mL/min, pore diameter: 1.9  $\mu\text{m}$ ), Pd/alumina powder catalyst (particle size: <25  $\mu\text{m}$ , 1 mg Pd) in slurry reactor (SR) and Pd/alumina egg shell catalyst (pellet size: 2–3 mm, thickness of the active shell: ca. 100  $\mu\text{m}$ , 1 mg Pd, circulation rate: 200 mL/min) in fixed bed reactor (FBR) at 50°C and 1 MPa hydrogen pressure.

[Color figure can be viewed in the online issue, which is available at [www.interscience.wiley.com](http://www.interscience.wiley.com).]

0.5–1 m, in a module to adjust the required membrane area. Because of the representative character of the single bundle, the setup is called a pilot plant here.

Figure 11a compares the results for COD conversion in lab scale with a single capillary and in the pilot plant with a bundle of 27 capillaries containing 30 mg Pd under similar conditions (50°C, 1 MPa, pore diameter: 1.9  $\mu\text{m}$ , mass flow per membrane area: 1.65 kg/m<sup>2</sup>s for the bundle, 1.48 kg/m<sup>2</sup>s for the single capillary membrane). The conversion curves for lab scale and pilot plant are in good agreement (Figure 11a). Also for the COE selectivity no significant difference was observed: the selectivity at complete conversion in the lab scale was 93% and in the pilot plant 94% (Figure 11b). The results demonstrate an easy scale up of the reactor system from lab to pilot scale by simple multiplication of the volume of the liquid phase, the membrane area and the circulation rate as the up scale factor.

Further experiments in the pilot plant validated the trends observed with a single tube in the lab scale. A higher circula-

tion flow rate of the reaction mixture through the membrane increased the conversion rate. Space-time-yields (STY) related to the module volume and to the Pd amount, respectively, were calculated at a COD-conversion of 95%. The highest STY was obtained with the highest circulation flow rate of 1.65 kg/(m<sup>2</sup> s). The STY was 1.1 mol/(m<sup>3</sup> module volume s) and 5.5 mol/(g<sub>Pd</sub> s), respectively in this case. The selectivity for COE was hardly affected; it remained in the range of 92–94% at complete conversion.

## Discussion

The effects of the main process variables and design parameters studied, e.g. the circulation flow rate, the nominal pore size and the Pd amount, on the activity and selectivity of the catalytic membranes in PFT mode can be explained straightforward in most cases.<sup>21</sup> However, the analysis of the experimental data with the simulation model showed some deviations which call for further investigations.

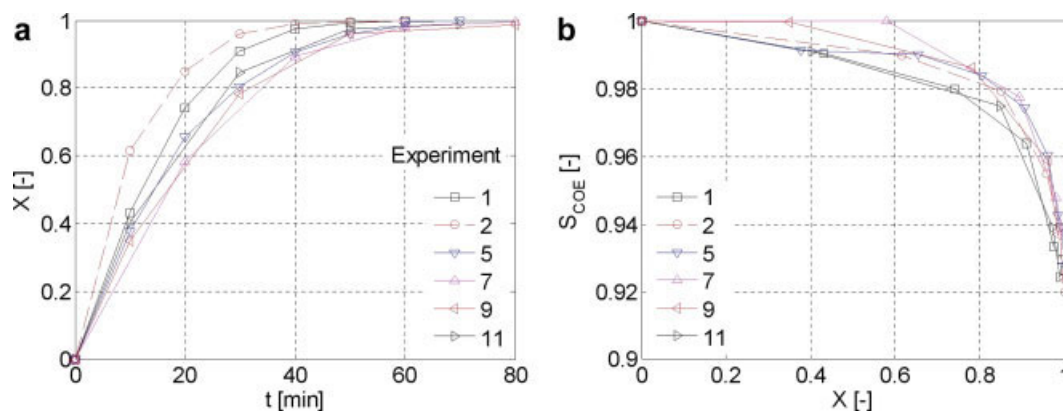


**Figure 10.** COD-conversion (a) and COE-selectivity (b) for a series of 11 experiments under the same conditions (50°C, 1 MPa H<sub>2</sub>-pressure, 5 vol % COD, circulation rate: 200 mL/min, Pd loading 1  $\pm$  0.1 mg Pd, pore size: 1.9  $\mu\text{m}$ ).

[Color figure can be viewed in the online issue, which is available at [www.interscience.wiley.com](http://www.interscience.wiley.com).]



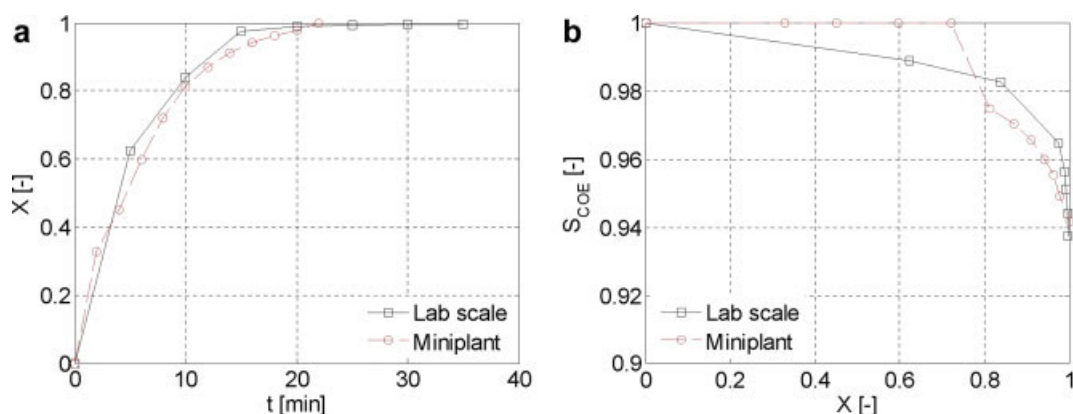


**Figure 11. COD-conversion (a) and COE-selectivity (b) for in lab scale and pilot plant (50°C, 1 MPa, 1.9  $\mu\text{m}$  pore diameter, 5 vol % COD, membrane flux: 1.65 (pilot plant) and 1.48  $\text{kg}/\text{m}^2 \text{ s}$  (lab scale)).**

[Color figure can be viewed in the online issue, which is available at [www.interscience.wiley.com](http://www.interscience.wiley.com).]

With increasing circulation rate (Figure 5), the residence time of the reactants in the membrane pores decreases, and so the fraction of hydrogen consumed per passage is lower. This gives a higher average hydrogen concentration within the membrane and consequently an increased overall reaction rate. As evident from Figure 5, the model shows a good agreement for the COE selectivity vs. the conversion of COD, but predicts lower reaction rates than found by experiments and also a more modest increase of the conversion rate with increasing circulation rate. The scattering of the preparation results, especially concerning the reproducibility of the active surface, is viewed as the major reason for the deviation between experiment and model. It should be noted, though, that for the simulation of the membrane reactor, a kinetic model derived from slurry reactor experiments with a different  $\text{Pd}/\alpha\text{-Al}_2\text{O}_3$  powder catalyst<sup>18</sup> was used without any fitting of the parameters. Notwithstanding the positive effect of the circulation flow rate on the performance of the system, the adjustable flow rate is limited by the applied pump and the membrane pore size, as both parameters control the pressure buildup at the membrane (Figure 6). Here, a compromise between operation costs and achievable STY must be found.

As mentioned earlier, the simulation with a two-dimensional model suggested no influence of the diffusion from the center of the pore to the pore wall on the reaction rate for the chosen conditions (e.g., pore size, flow rate, pressure and temperature as well as reaction kinetics). Consequently, the predicted curves in Figure 7 (lines) do not vary with the pore size. They agree well with the experimental data obtained for 1.9 and 3.0  $\mu\text{m}$  pore diameter, but the membrane with 0.6  $\mu\text{m}$  nominal pore size was clearly more active than those two. Moreover, it was also more active than predicted by the simulation based on the known Pd amount. In our previous work,<sup>2</sup> an increase of the reaction rate was found for partial hydrogenation reactions on polymer membranes with pore diameters decreasing from 0.4 to 0.1  $\mu\text{m}$ . These observations were explained by better contact between the reactants and the catalyst in smaller pores. In larger pores, a part of the reactants flows through in a kind of bypass with fewer contacts to the catalyst at the pore wall. Yet in view of the simulation results shown in Figure 7, this seems unlikely for the experimental conditions applied here. Furthermore, TEM analyses (Table 1) showed

no significant change of the Pd crystallite size with the membrane pore size, so other explanations must be considered, for example an inhomogeneous distribution of the Pd in pores with different diameter.

The experimentally observed effect of the Pd amount on the activity (Figure 8) also is reproduced only in part by the simulation model. Whereas the results for the membrane with the intermediate Pd content of 1 mg are nicely matched, the predicted influence of the Pd loading is weaker than found in the experiment, both for higher and for lower Pd contents. As shown in Figure 12, the predicted concentration change of hydrogen over the the membrane is still moderate even for the highest Pd loading of 1.5 mg, e.g., from about 65.5 to 54.5  $\text{mol}/\text{m}^3$ , which results in an expected increase of the reaction rate almost proportional to the Pd amount. A pronounced difference in the hydrogen concentration profile for the three different catalyst loadings can be excluded,

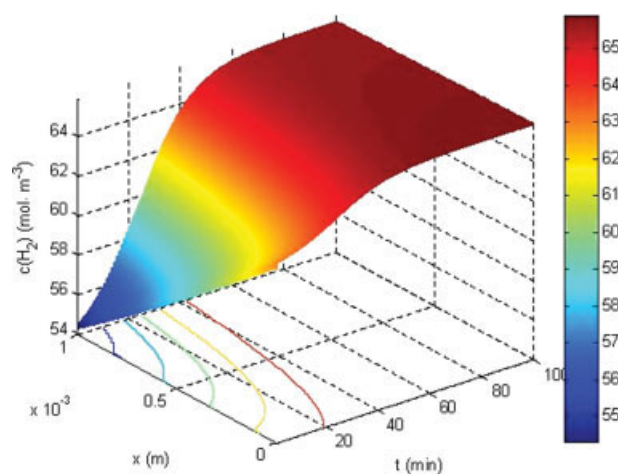


**Figure 12. Simulated  $\text{H}_2$  concentration profiles through the membrane as a function of time for a Pd loading of 1.5 mg (50°C, 1 MPa  $\text{H}_2$  pressure, pore size: 1.9  $\mu\text{m}$ , circulation rate: 200  $\text{mL}/\text{min}$ ).**

[Color figure can be viewed in the online issue, which is available at [www.interscience.wiley.com](http://www.interscience.wiley.com).]

since even with the highest loading of 1.5 mg there is only a weak decay of the hydrogen concentration from 65.5 to 54.5 mol/m<sup>3</sup>. A nonlinear dependence of the Pd surface area on the Pd loading, i.e., smaller Pd crystallites for higher Pd loadings and vice versa, would be a possible explanation which, however, would need confirmation by additional characterization.

Comparing the results obtained with the catalytic membranes to those with the powder catalyst in the slurry reactor (Figure 10) reveals that the reaction in the membrane runs under microkinetic control when the circulation flow rate is high enough. Consequently, the maximum (intrinsic) selectivity is reached. The simulation of the reaction in the egg-shell catalyst suffers from the high sensitivity of the results with respect to the thickness of the active shell. An inhomogeneous thickness or inhomogeneous dispersion of the Pd within the active shell can easily account for the deviation of the simulated from the measured reaction rate. The model reproduces the marked decrease of the COE selectivity with increasing conversion for the egg shell catalyst, but tends to predict higher selectivity at complete conversion. Moreover, for the powder catalyst in the slurry reactor a higher activity is predicted compared to the experimental results, whereas for the membrane the predicted activity is lower than experimentally observed. It should be stated again, though, that the simulation is based on the kinetics determined from the results of separate experiments with a powder Pd/ $\alpha$ -Al<sub>2</sub>O<sub>3</sub> catalyst in a slurry reactor<sup>18</sup> without any fitting of the parameters.

The results, altogether, make clear that although being designed for this type of reaction, the egg shell catalyst is nevertheless affected by some pore diffusion limitation that results in a weak performance with respect to the selectivity of the reaction, whereas this is negligible in the catalytic membrane in PFT-mode.

For a process to produce 1 ton/h of a product by a partial hydrogenation with a similar kinetics than COD hydrogenation, an overall volume of 2–10 m<sup>3</sup> would be required, depending on a suitable reactant concentration. This solution would be circulated through a membrane module with 60 m<sup>2</sup> of porous alumina membrane containing 20 g of palladium. The volume of this membrane module would be about 1 m<sup>3</sup>. For an economic evaluation, this process has to be compared with a standard batch reactor with dispersed catalyst pellets. The additional costs for the ceramic membrane should be more than compensated by a reduction of the costs for the reactant because of the improved selectivity and for palladium because of the higher activity.

## Conclusion

The partial hydrogenation of COD was studied for evaluating the potential to increase the activity and selectivity of a three-phase reaction by making use of the properties of a catalytic membrane in PFT operation mode. The reaction rate was mainly affected by the Pd amount and the circulation flow rate through the membrane. The selectivity for COE was not affected by these parameters; it was always in the range of 92–95% when COD was completely converted. This indicates that the reaction in the membrane reactor was unaffected by mass transfer limitations as it is obtained under microkinetic control with a powder catalyst.

Already with the lowest circulation flow rate applied in the membrane module, the removal of COE out of the membrane pores and its replacement by COD occurs sufficiently fast and no depletion of COD accompanied by an accumulation of COE decreased the selectivity of the partial hydrogenation of COD. The consecutive reaction to COA does not occur until the COD concentration in the reaction mixture is very low because the adsorption of COD ( $K_{ad} = 17 \text{ L mol}^{-1}$ ) at the catalyst is stronger than of COE ( $K_{ad} = 10 \text{ L mol}^{-1}$ ). This difference in adsorption constants is caused by the conjugated double bond system of COD that allows stronger surface interaction than a single double bond. As long as only COD is adsorbed at the catalyst, no COE is hydrogenated to COA.

With the membrane reactor, higher selectivity was obtained compared to conventional egg shell catalyst in a fixed-bed reactor. Scale up from lab scale to a pilot plant is possible with comparable performance of the catalyst. STY can be optimized by applying a sufficiently high circulation flow rate through the membranes. By pumping the reaction mixture at a higher circulation rate through the reactor system, more passages per time occur and a complete conversion of the reactants will need less time. The minimum number of circulations needed for complete conversion is defined by the ratio of the initial concentration of the substrate and the saturation concentration of hydrogen (if one mole of substrate reacts with one mole of hydrogen). This minimum number cannot be realized because the hydrogen concentration within the membrane decreases below the saturation concentration during every passage.

The performance of the membrane reactor can be predicted using a model based on the material balance of the reactor system of saturation vessel and membrane module. It includes the intrinsic kinetics of the reaction, the gas liquid mass transfer and the convective flow of the reaction mixture through the membrane pores. For further optimization, the model will be used for calculation of the concentration profiles of the reactants within the membrane. Optimal utilization of the Pd and the whole membrane module should result in high STY if strongly decaying concentration profiles of the reactants across the membrane can be avoided. The next steps will be an investigation of reactions with other substrates, metals as catalyst and supports in the membrane reactor in forced-through-flow mode in order to evaluate the application potential.

## Acknowledgments

This work was supported by Federal Ministry for Education and Research (BmBF), Germany.

## Literature Cited

- Schomäcker R, Schmidt A, Frank B, Haidar R, Seidel-Morgenstern A. Membranen als Katalysatorträger. *Chem Ing Technol.* 2005;5:77.
- Schmidt A, Haidar R, Schomäcker R. Selectivity of partial hydrogenation reactions performed in a pore-through-flow catalytic membrane reactor. *Catal Today.* 2005;104:305–312.
- Purnama H, Kurr P, Schmidt A, Voigt I, Wolf A, Warsitz R, Schomäcker R.  $\alpha$ -Methylstyrene Hydrogenation in a Flow-Through Membrane Reactor. *AIChE J.* 2006;52:2805–2811.
- Torres M, Sanchez J, Dalmon JA, Bernauer B, Lieto J. Modeling and simulation of a three-phase catalytic membrane reactor for nitrobenzene hydrogenation. *Ind Eng Chem Res.* 1994;33:2421–2425.

5. Peureux J, Torres M, Mozzanega H, Giroir-Fendler A, Dalmon JA. Nitrobenzene liquid-phase hydrogenation in a membrane reactor. *Catal Today*. 1995;25:409–415.
6. Vitulli G, Verrazzani A, Pitzalis E, Salvadori P. Pt/ $\gamma$ -Al<sub>2</sub>O<sub>3</sub> catalytic membranes vs. Pt on  $\gamma$ -Al<sub>2</sub>O<sub>3</sub> powders in the selective hydrogenation of *p*-chloronitrobenzene. *Catal Lett*. 1997;44:205–210.
7. Reif M, Dittmeyer R. Porous, catalytically active ceramic membranes for gas-liquid reactions: a comparison between catalytic diffuser and forced through flow concept. *Catal Today*. 2003;82:3–14.
8. Lange C, Storck S, Tesche B, Maier WF. Selective hydrogenation reactions with a microporous membrane catalyst, prepared by sol-gel dip coating. *J Catal*. 1998;175:280–293.
9. Tilgner IC, Lange C, Schmidt HW, Maier WF. Three-phase hydrogenations with microporous catalytic membranes. *Chem Eng Technol*. 1998;21:565–570.
10. Lambert CK, Gonzalez R. Activity and selectivity of a Pd/ $\gamma$ -Al<sub>2</sub>O<sub>3</sub> catalytic membrane in the partial hydrogenation reactions of acetylene and 1,3-butadiene. *Catal Lett*. 1999;57:1–7.
11. Dittmeyer R, Höllein V, Daub K. Membrane reactors for hydrogenation and dehydrogenation processes based on supported palladium. *J Mol Catal A: Chem*. 2001;173:135–184.
12. Vincent MJ, Gonzalez RD. Selective hydrogenation of acetylene through a short contact time reactor. *AIChE J*. 2002;48:1257–1267.
13. Bottino A, Capannelli G, Comite A, Del Borghi A, Di Felice R. Catalytic ceramic membrane in a three-phase reactor for the competitive hydrogenation-isomerization of methylenecyclohexane. *Sep Pur Technol*. 2004;34:239–245.
14. Dittmeyer R, Svajda K, Reif M. A review of catalytic membrane layers for gas/liquid reactions. *Top Catal*. 2004;29:3–27.
15. Gröschel L, Haidar R, Beyer A, Cölfen H, Frank B, Schomäcker R. Hydrogenation of propyne in palladium-containing polyacrylic acid membranes and its characterization. *Ind Eng Chem Res*. 2005;44:9064–9070.
16. Fritsch D, Kuhr K, Mackenzie K, Kopinke FD. Hydrochlorination of chloroorganic compounds in ground water by palladium catalysts. I. development of polymer-based catalysts and membrane reactor tests. *Catal Today*. 2003;82:105–118.
17. Khassin AA, Sipatov AG, Yurieva TM, Chermashentseva GK, Parmon VN. Plug-through contactor membranes (PCM) for the Fischer-Tropsch synthesis. *Prepr Pap Am Chem Soc Div Pet Chem*. 2004;49:175–178.
18. Schmidt A, Schomäcker R. Kinetics of 1,5-Cyclooctadiene Hydrogenation on Pd/ $\alpha$ -Al<sub>2</sub>O<sub>3</sub>. *Ind Eng Chem Res*. 2007;46:1677–1681.
19. Press WH, Teukolsky SA, Vetterling WT, Flannery BP. *Numerical Recipes in Fortran. The Art of Scientific Computing*, 2nd ed. Cambridge, MA: Cambridge University Press, 1994. Chapter 16.2.
20. Frusteri F, Parmaliana A, Ostrovskii NM, Iannibello A, Giordano N. Selective oxidation of ethylene over carbon-supported Pd and Pt catalytic membranes. *Catal Lett*. 1997;46:57.
21. Fritsch D, Randjelovic I, Keil F. Application of a forced-flow catalytic membrane reactor for the dimerisation of isobutene. *Catal Today*. 2004;98:295–308.

Manuscript received Dec. 6, 2006, and revision received Oct. 21, 2007.